ARTICLE OPEN

Check for updates

High-throughput screening of zwitterion-based coatings towards improved mechanical stability and drug-loading capacity

Jingzhi Yang[1,2,6], Yami Ran[1,2,3,6], Luyao Huang[4], Chenhao Ren[1,2], Xiangping Hao[2,5], Lingwei Ma[1,2] and Dawei Zhang[1,2,3]✉

2-hydroxyethyl methacrylate (HEMA), poly(ethylene glycol) (PEG), and zwitterionic polymers are currently considered the most extensively studied antifouling hydrogel coatings. However, systematic identification of these coatings to unleash their potential properties is tremendously under-represented. Here, we report a high-throughput optimizing strategy that combines highly miniaturized hydrogel synthesis and screening to fine design zwitterion-based hydrogel coatings. Compared with the traditional one-by-one synthesis and characterization methods, the proposed high-throughput strategy accelerated the discovery of candidate materials with a high-efficiency and cost-effective approach. To tailor multiple parameters of coatings, 1575 unique coating combinations with continuous gradients were prepared only required 600 µL reactant. The mechanical stability and drug-loading capacity of the coating spots were sequentially evaluated via immersion swelling, flow, tape-peeling, and dye-retaining tests. This strategy could efficiently reveal the composition/structure-function relationships of the hydrogel coatings and also other materials, which is promising for the rapid screening and design of desired implantable device surfaces.

npj Materials Degradation (2023)7:51 ; https://doi.org/10.1038/s41529-023-00362-5

INTRODUCTION

Biomedical materials play a crucial role in the survival and well-being of patients. Owing to their decent mechanical properties, corrosion resistance and biocompatibility, stainless steels are widely used for implantable medical devices. However, these devices are susceptible to pathogenic bacterial contamination and result in severe biofouling[1,2]. Biofouling on the surface adversely affects both patient care and implant inertness[3,4]. Preventing biological contamination has become one of the greatest challenges for all biomedical applications. According to a survey by the World Health Organization, healthcare-associated infections (HAIs) have resulted in up to 40,000 fatalities annually[5]. Fabricating a highly hydrophilic antifouling coating on implantable devices can effectively mitigate the biofouling damage. Hydrogels are great candidates for antifouling materials because of the strong hydrophilicity and water retention as well as the high drug-loading capacity[6,7]. As classic hydrogel materials, antifouling polymer systems based on 2-hydroxyethyl methacrylate (HEMA), polyethylene glycol (PEG), and zwitterion have been well demonstrated[8–10].

Zwitterionic polymers were inspired by phosphorylcholine headgroups abundant in cell membranes[11,12], containing both anionic and cationic groups in their repeating units. They can lower the mobility of the water layer and exhibit a stronger repulsive force against biofouling[13]. Meanwhile, zwitterionic segments are known to increase the swelling ratio of hydrogels[14]. However, their application was limited by the unsatisfying adhesive and mechanical stability. Several methods have been devised to enhance the stability of zwitterionic coating on different kinds of substrates. Gong et al.[15] produced a doubly biomimetic copolymer PMNC with dopamine on the side chain, and the PMNC copolymers were fixed on the different surfaces by increasing the dopamine side chain. Huang et al.[16] composed three zwitterionic-phosphonic random copolymers by two methacrylate monomers, which include phosphonate and phosphonic pendants and then immobilized these zwitterionic copolymers on Ti alloy plate via the strong coordination interaction between metallic substrates and phosphonate/phosphonic motifs. However, the introduction of adhesion motifs would compromise the intrinsic antifouling performance of the zwitterionic hydrogel. HEMA polymers were widely used for antifouling materials and were reported to have good elastic properties[17]. Furthermore, copolymerizing HEMA was promising to improve the toughness and strength of mechanically poor hydrophilic hydrogel[18]. Therefore, the combination of zwitterions and HEMA segments, as well as optimization of the synthesis parameters, holds great promise to develop antifouling hydrogel coatings with desirable mechanical stability and swelling capacity. The existing studies have shown that monomer content[19], degree of crosslinking[20] and ratios of functional groups[21] all have an impact on the polymerization and final properties of the hydrogel coatings. Screening combinations of such a diverse range of variables and potentially available precursor compounds demands high time- and resource- consumption that traditional one-by-one synthesis and evaluation experiments can hardly achieve. A rapid and cost-effective platform is urgently required to accelerate the development of zwitterion/HEMA hydrogels and unleash the true potential of these known materials.

High-throughput technologies achieve new insights into materials development by exploring thousands of materials

[1]Beijing Advanced Innovation Center for Materials Genome Engineering, Institute for Advanced Materials and Technology, University of Science and Technology Beijing, 100083 Beijing, China. [2]National Materials Corrosion and Protection Data Center, University of Science and Technology Beijing, 100083 Beijing, China. [3]BRI Southeast Asia Network for Corrosion and Protection, Shunde Graduate School of University of Science and Technology Beijing, 528000 Foshan, China. [4]State Key Laboratory of Advanced Power Transmission Technology, State Grid Smart Grid Research Institute Co., Ltd., 102209 Beijing, China. [5]School of Materials Science and Engineering, University of Science and Technology Beijing, 100083 Beijing, China. [6]These authors contributed equally: Jingzhi Yang, Yami Ran. ✉email: dzhang@ustb.edu.cn

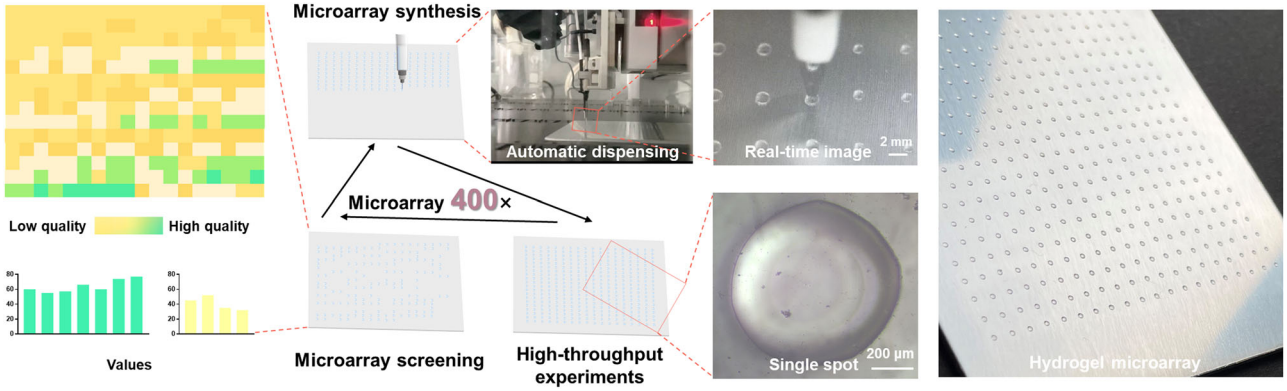

Fig. 1 Schematic diagram showing the preparation of 400 hydrogel coatings in high-throughput methodology. The single substrate was spotted with a 20 × 20 droplet microarray.

combinations via simultaneous synthesis and investigation. Recently, this method has raised great attention in the development of drug mixtures, antibacterial compounds and biomaterial surfaces[22,23]. Levkin's group[24] employed a miniaturized high-throughput droplet microarray (DMA) system for the immediate screening of antibacterial compounds. Based on DMA slides, the nanoliter-sized droplet microarrays containing bacteria were prepared to rapidly investigate the drug resistance of *P. aeruginosa*. Fang et al. [25] proposed a high-throughput strategy based on gradient surfaces to screen the optimized parameters for preparing mono and dual peptides functionalized Ti surfaces with exceptional biocompatibility and antimicrobial activity. In these examples, the optimal materials design with enhanced particular properties could be facilitated by exploring a much larger range of chemical spaces. Thus, the materials composition/structure-function relationships could be easily forecasted and better understood.

In this work, we described a high-throughput strategy whereby combinatorial libraries of small molecules with continuous gradients were highly miniaturized synthesized and directly investigated. This strategy achieved a high-efficiency and cost-effective method to discover the optimized parameters for preparing the sulfobetaine methacrylate (SBMA)/HEMA antifouling hydrogel coatings with ideal mechanical stability and drug-loading capacity. The stability of hydrogel microarrays was sequentially investigated after immersion swelling, flow and tape-peeling damages. The hydrogel microarrays were imaged after staining in a Congo red solution to evaluate their drug-loading capacity.

RESULTS AND DISCUSSION

Hydrogel microarray preparing

In this work, we claimed a high-efficiency and cost-effective method to produce a huge number of hydrogel spots in one substrate (Fig. 1). The hydrogel microarray we prepared provided the possibility for rapid identification of coatings with various synthesis parameters. To implement the high-throughput combinatorial manner, we used an automated droplet microarray printer to generate high-quality droplets with a continuous gradient in reactant content. The printer based on a non-contact picoliter liquid-dispensing technology was equipped with piezoelectric pipetting tips for well-controlled drop bursts. This non-contact printer could offer real-time image feedback to supervise the dispensing process, thus allowing the high-precise dosage of droplets. Moreover, high-viscosity liquids could also be dispensed by a heating module, which significantly improved the versatility of the printer. Generally speaking, the preparation of one hydrogel microarray was equivalent to performing hundreds of traditional one-by-one synthesis experiments in vials. This high-throughput approach had great advantages in the rapid preparation of coatings with different compositions and could greatly reduce the dose requirements of polymerization.

Zwitterionic polymers were popular for their excellent antifouling performance and high water content, but their coatings were limited by the lack of stability on material surfaces. The introduction of HEMA segments has been reported to improve the mechanical properties of zwitterionic hydrogels[26]. However, few studies were found focusing on the performance of hybrid SBMA/HEMA hydrogel coatings. We aimed to use high-throughput technology to construct SBMA/HEMA hydrogel coating libraries, study on the feasibility of our strategies, and optimize the synthesis parameters of the coatings, thus accelerating the discovery of hydrogel coatings with desirable stability and drug-loading capacity. To achieve this, we used the non-contact liquid-dispensing technology to create a hydrogel coating microarray consisting of 315 unique polymer spots (Fig. 2). Polymer synthesis was achieved by sequentially depositing the reactants to the same spot on a drop-by-drop basis (details were presented in "Methods"). The whole process was executed in 1260 (315 × 4) pipetting steps, and only requires 10 min and less than 40 μL of reagent in total (~120 nL for each spot). Considering the cost of time and resources, a traditional one-by-one manner could hardly construct a similar library.

The homogeneity of hydrogel coating spots

A representative hydrogel coating spot generated via the automated printer was used to confirm the adequate mixing of multiple reactant droplets. As shown in Fig. 3a, overprinted droplets burst from the pipetting tips impacted on the pre-printed droplets, inducing an obvious vortex that facilitated the proper mixing of the droplet on the substrate. To further identify the mixing behavior of the reagents during the printing process, we used Raman spectroscopy measurements and fluorescent dye treatments on a representative hydrogel coating spot to verify the homogeneous distribution of components within the droplet (details were presented in "Methods"). As shown in Fig. 3b, four peaks centered at 1034, 1456, 1732 and 2911 cm^{-1} are attributed to S=O, CH_3/CH_2, carbonyl, as well as C–H stretching vibrations of the HEMA/SBMA hydrogel spot, respectively. We used the Raman mapping tests to investigate the distribution of these four representative vibrations and export the results in different colors. As shown in Fig. 3e, f, the mapping of the selected vibrations was all distributed radially even. The higher intensity of vibrations toward the center of the hydrogel spot, which indicated more abundant functional groups, was attributed to the bulged shape of the spot. Finally, the printed droplets were stained with fluorescein/rhodamine B to ensure the reagents reacted

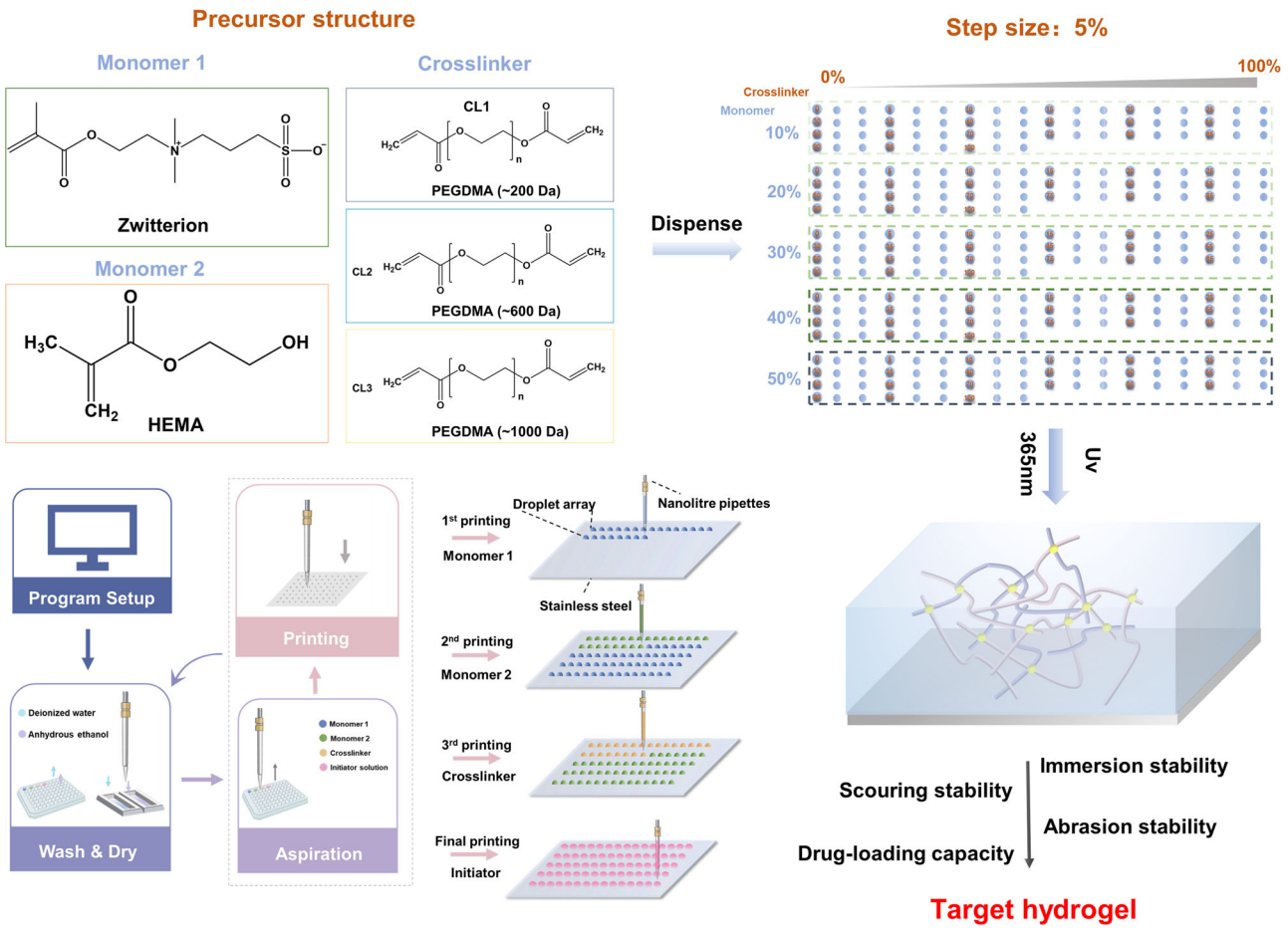

Fig. 2 Schematic diagram showing the hydrogel microarray preparation process. The monomer content was 10%, 20%, 30%, 40%, and 50% by weight. The crosslinker PEGDMA was deposited to these monomers in concentrations ranging from 0%–100% (weight percent of monomer); the step size of the concentrations was 5%. Red numbers in blue circles represent the specific concentration of the printed crosslinker. The diameter of each hydrogel spot was ~1 mm, the distance between the hydrogel spots was ~2 mm.

throughout the whole volume. As shown in Fig. 3g, h, the even distribution of the fluorescent dyes was demonstrated in the green and red fluorescence intensity images. The significant vortex induced by overprinting droplets may contribute to the adequate mixing of fluorescent dye. Overall, the real-time image, Raman spectroscopy, and fluorescence measurements confirmed the adequate mixing and homogeneous distribution of the reactants in the hydrogel via the high-throughput synthesis manner. Our strategies enable rapid production of picoliter-size hydrogel coatings that are similar to that synthesized by conventional methods.

The immersion swelling tests of hydrogel microarrays

Zwitterionic hydrogels were well known for the excellent swelling properties, but their inadequate mechanical properties may easily lead to the detachment of swollen hydrogel coatings from the substrate[27–30]. Therefore, mechanical stability is of great significance for antifouling hydrogel coatings. To achieve a rapid and rational design of zwitterion-based hydrogel coatings with optimized immersion stability, we synthesized 15 hydrogel coating microarrays (each microarray consisted of 315 unique spots) including multiple parameters such as monomer compositions, monomer contents, crosslinker contents and crosslinker molecular weights. Then, the as-prepared SBMA/HEAM hydrogel coating microarrays were directly immersed in PBS solution for 72 h to allow the hydrogel spots to fully swell. The immersion stability of hydrogel coatings spots was determined by the damage degree after immersion swelling tests, and the results were summarized in heat maps (Fig. 4b–d). The deepest blue represents the fully stable spots that remained intact after immersion for 72 h. The representative optical images of intact spots, slightly damaged spots, seriously damaged spots and spots that were completely removed were presented in Supplementary Fig. 1. The heap map results indicated the introduction of HEMA significantly improved the stability of the zwitterionic hydrogels. No intact spots are visible without the involvement of HEMA segments. Hydrogel coatings made of SBMA without HEMA could highly swell in PBS solutions but they were too fragile to resist large deformation. With the HEMA content increasing, stable spots (highlighted with the deepest blue color) started to be visible in hydrogel coating microarrays.

Comparing each column in Fig. 4b, c and d, it is clear that the performance of hydrogels with high molecular-weight PEGDMA crosslinkers is generally worse than that of the hydrogels with low molecular-weight crosslinkers. Among the three molecular weight crosslinkers we selected, the hydrogel coating spots exhibited the most stability with the crosslink of PEGDMA (Mn ~200). These results may attribute to that the length of the crosslinker molecules could impact the interaction induced between pendant functional groups in the hydrogel network. Using short length crosslinker makes pendant functional groups close enough to contact each other and interact when the hydrogel coatings deform during immersion tests. These interactions create a local friction area that would dissipate energy under deformation[18].

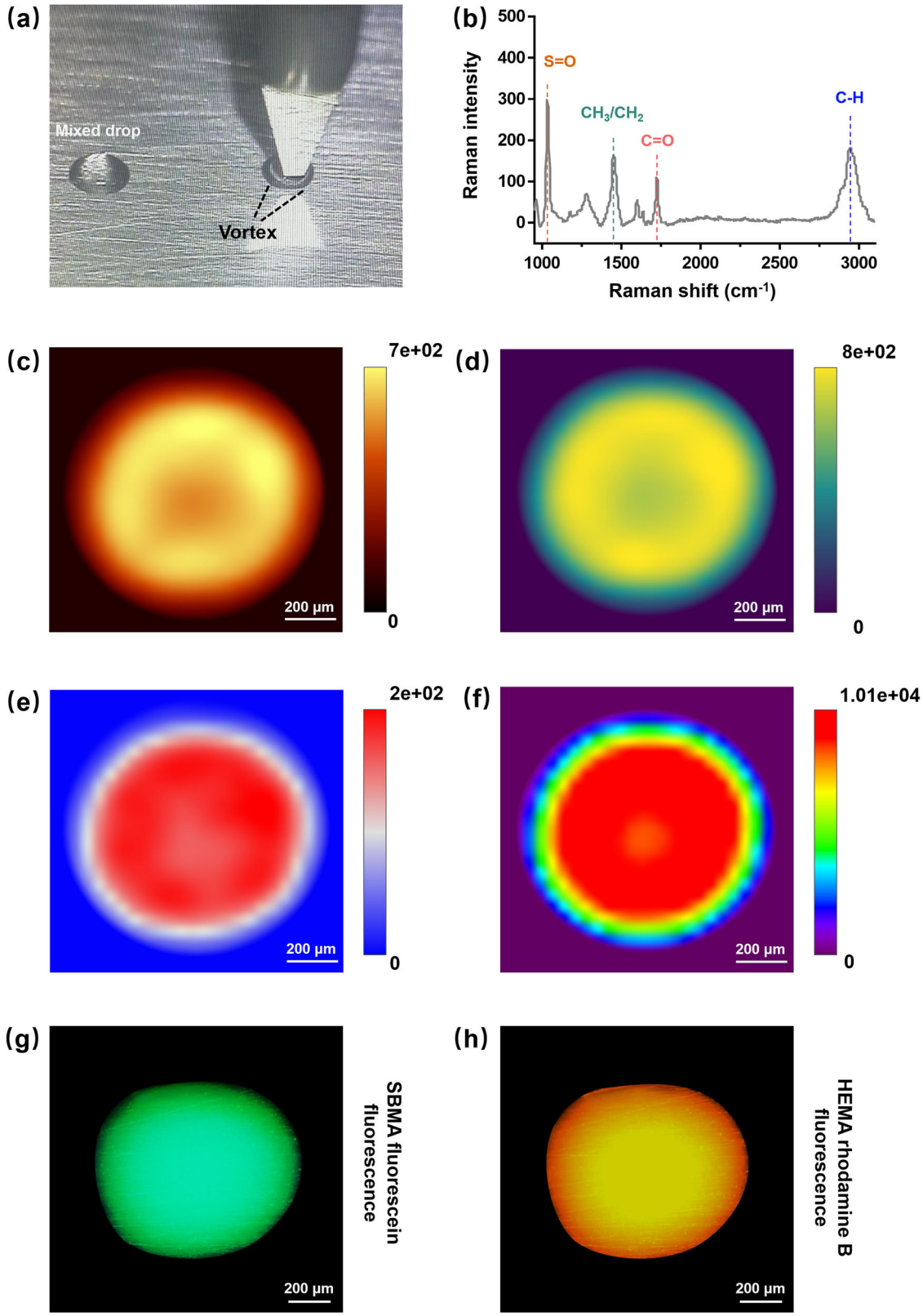

Fig. 3 The homogeneity proving of hydrogel coating spots. a The real-time image of the droplet mixing process. **b** Raman spectrum of the representative hydrogel coating spot. Raman mapping of **c** S=O vibration; **d** CH_3/CH_2 vibration; **e** C=O vibration and **f** C–H vibration on a representative hydrogel coating spot. **g** Green and **h** red fluorescence intensity image of a representative hydrogel coating spot.

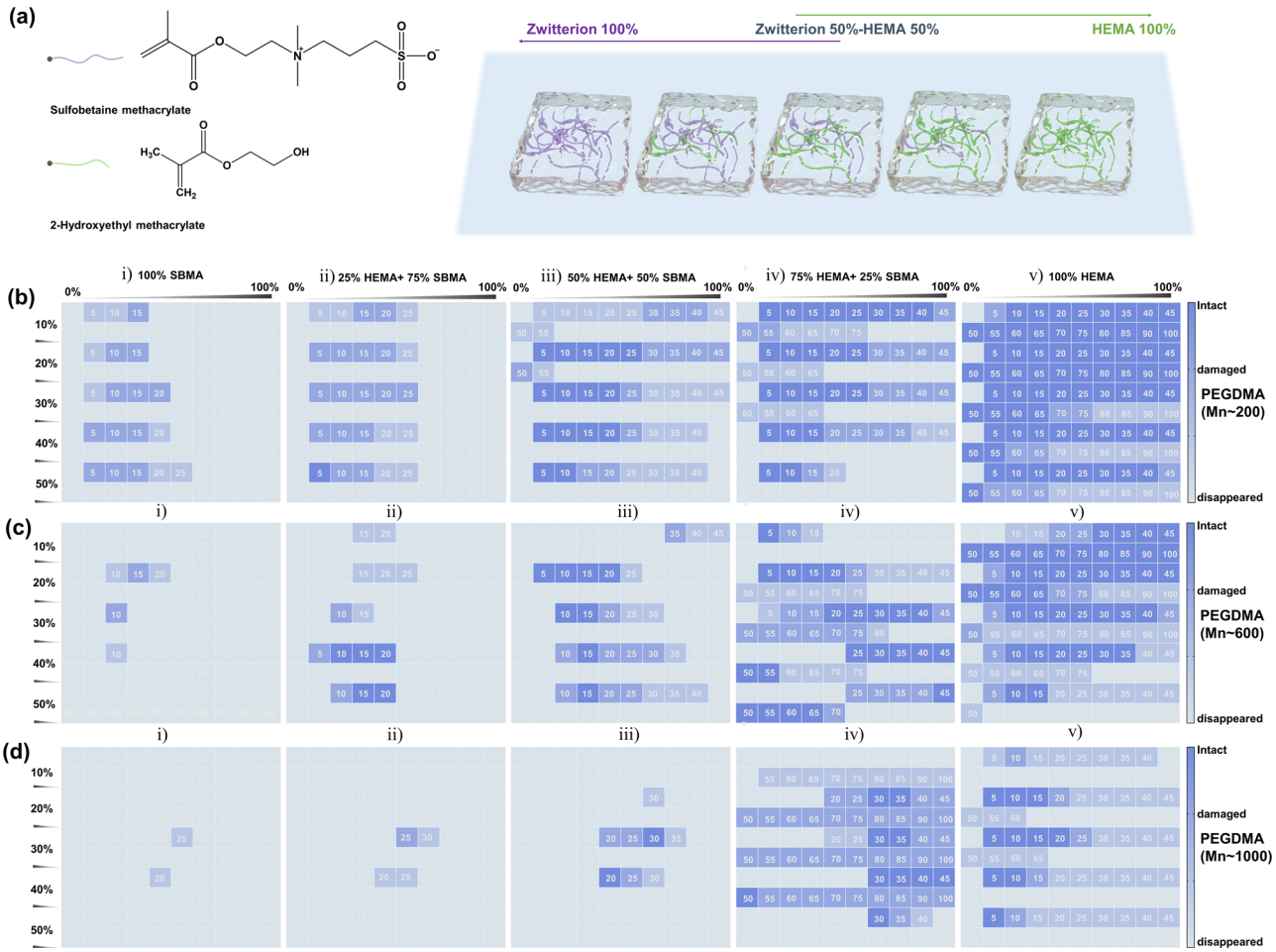

Fig. 4 The immersion swelling test results of the hydrogel microarrays via a high-throughput manner. a Schematic diagram showing the hydrogel coatings composed of zwitterion (SBMA, purple) and 2-Hydroxyethyl methacrylate (HEMA, green) monomers with PEGDMA crosslinker. Heat maps of the stability of hydrogel coatings synthesized by crosslinkers **b** PEGDMA (Mn ~200), **c** PEGDMA (Mn ~600) and **d** PEGDMA (Mn ~1000) in still PBS solution based on high-throughput screening assays. We evaluated five monomer compositions, including (i) 100% SBMA, (ii) 25% HEMA + 75% SBMA, (iii) 50% HEMA + 50% SBMA, (iv) 75% HEMA + 25% SBMA, (v) 100% HEMA. The numbers (white) inside the heat maps represent the crosslinker contents (wt.%); the numbers on the left of the heat maps represent the monomer contents (wt.%); the depth of color represents the different damage degrees of hydrogel coatings after the immersion swelling test.

Moreover, these strong interactions may activate the internal hydrogen bond between hydroxyl groups, which also enhanced the toughness of polymer hydrogels[31–33]. Longer crosslinkers would weaken these interactions, resulting in fewer stable coatings in hydrogel coating microarrays (evidenced by the smaller number of deepest blue squares visible in heat maps). Tailoring the molecular length of crosslinker allows us to optimize the mechanical stability of these hydrogel coatings.

We also evaluated a library of SBMA/HEMA hydrogel coatings with a wide range of crosslinker contents (totaling 21 different concentrations from 0–100 wt.% with respect to monomers). In polymer hydrogel networks, the crosslinking density plays a crucial role in mechanical stability. All the uncrosslinked hydrogel spots disappeared after immersion in the absence of crosslinkers. Furthermore, lower usage of the crosslinker would lead to insufficient elastic properties of the polymer network, which can hardly ensure the stability of hydrogel coatings. When excessive crosslinkers are used, the hydrogel coatings may become too fragile to remain intact when against swelling damage[34]. As expected, these results were reproduced from the heat maps (Fig. 4b). The color depth of the squares does not always increase monotonously with the higher amount of crosslinker. Some of the deepest blue squares are located in the middle of the selected range, corresponding to moderate crosslinking densities.

The monomer content also actually impacts the distribution of the squares with different depths of blue color. Typically, progressively substituting HEMA with SBMA rendered the hydrogels more stable in higher monomer content. Besides, a similar trend was available when substituting a low molecular weight crosslinker with a higher one[29,35,36]. Benefiting from the production of hydrogel coating microarrays, we easily obtained the relationship between the synthesis parameters of hydrogel coatings and their stability under immersion. In immersion swelling tests, 208 stable (out of the total 1575) hydrogel spots were discovered for the subsequent evaluation.

The flow and tape-peeling tests of hydrogel microarrays

Antifouling hydrogel coatings are likely to be collapsed and detached from the substrate due to the inevitable flushing and abrasion damages during and after implantation[21]. In order to further assess the mechanical stability of hydrogel coatings under more rigorous and practical settings, the hydrogel coating microarrays were fixed at the bottom of a glass tube, which was connected to a peristaltic pump. The peristaltic pump circulates PBS solution through the hydrogel coating microarrays to simulate an in vivo flushing condition. The flow rate was set at a constant 500 mL min^{-1} to simulate the practical blood flow rate in an artery

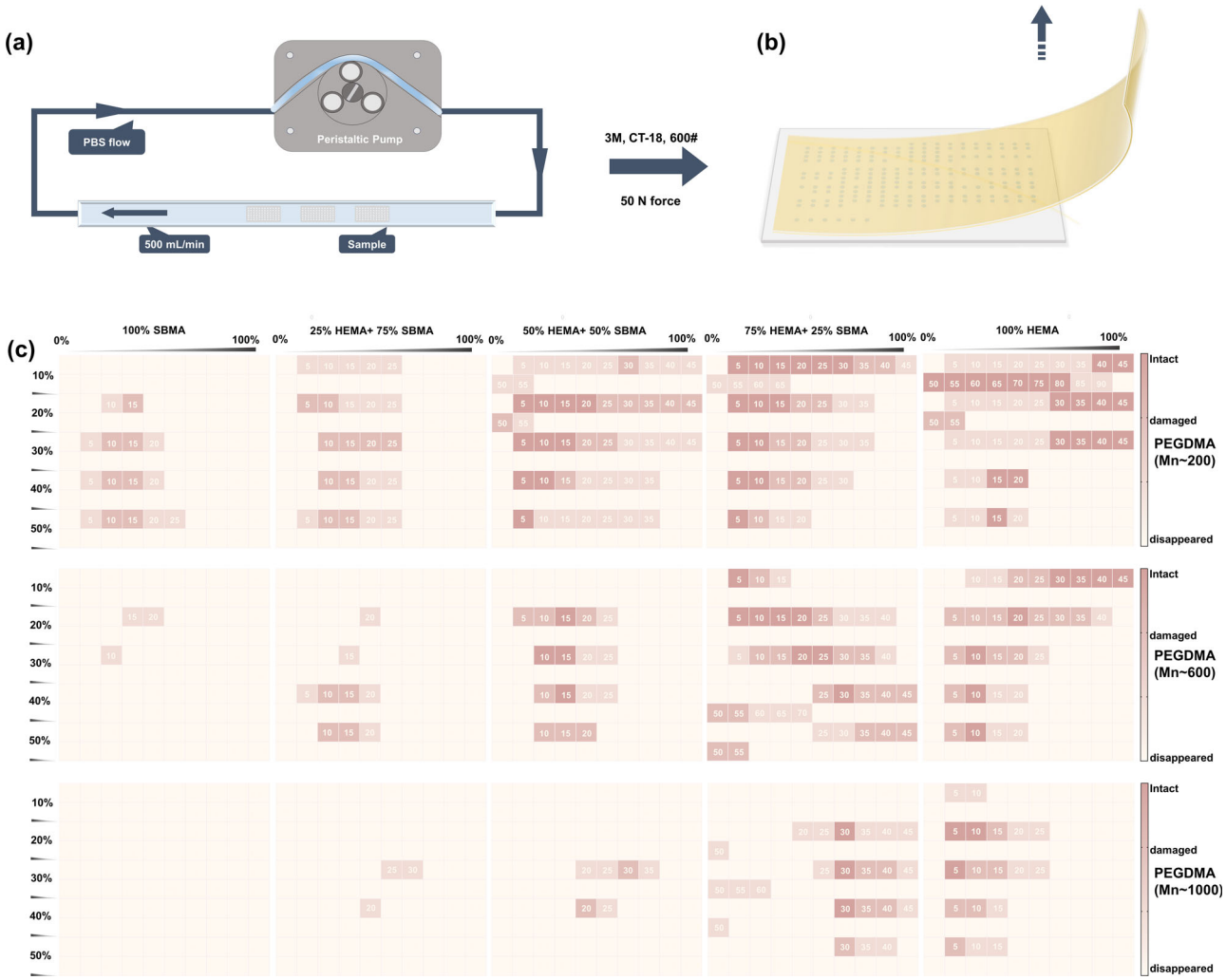

Fig. 5 The flow and tape-peeling test results of the hydrogel microarrays via a high-throughput manner. a Schematic diagram showing the method simulating the flushing treatment under in vivo conditions. **b** Schematic diagram showing the method simulating the abrasion treatment. **c** Heat maps of the stability of hydrogel coatings after flow and tape-peeling tests based on high-throughput screening assays. The numbers (white) inside the heat maps represent the crosslinker contents (wt.%); the numbers on the left of the heat maps represent the monomer contents (wt.%) the depth of color represents the different damage degrees of hydrogel coatings after flushing and abrasion tests.

(Fig. 5a)[37]. Following the exposure to the flowing conditions, we used tape-peeling tests to simulate the abrasion damage of hydrogel coatings (Fig. 5b)[38]. The damage degree of 208 hydrogel spots screened from the immersion swelling tests was directly evaluated via flow and tape-peeling tests. The experimental results were systematically summarized and exhibited in heat maps (Fig. 5c). Hydrogel spots with HEMA content of 0% or 25% could not resist the flow and tape-peeling damages and severely lost their integrity after 72 h of flow and 10 cycles of peeling. Similar to the results of immersion swelling tests in the section "The immersion swelling tests of hydrogel microarrays", increasing the HEMA monomer ratio or substituting a high molecular weight crosslinker with a relatively low one rendered the hydrogel spots more stable. Notably, hydrogel spots with HEMA content 100% suffered serious damage after flow and tape-peeling tests, while the number of intact spots in compositions HEMA: SBMA = 50%: 50% and 75%: 25% only reduced moderately. These results demonstrated the proper introduction of zwitterionic segments induced an improvement in the abrasion resistance of hydrogel coatings[30,39–41]. After these tests, we further narrowed the chemical space for screening antifouling hydrogel coatings with optimized stability. 70 stable (out of the total 1575) hydrogel spots stood out after immersion swelling, flow and tape-peeling tests.

The drug-loading capacity assays of hydrogel microarrays

Zwitterionic hydrogels are widely used as drug delivery systems due to their remarkable swellability. Swellability correlates positively with the drug-loading capacity of hydrogels[42]. We aimed to efficiently assess the swelling performance of each spot in the hydrogel coating microarray via a high-throughput manner and make the assessment results quantized. To do so, the hydrogel coating microarrays were immersed in Congo red solution for 24 h to allow the hydrogel spots to fully swell and retain the dye to the maximum levels. Therefore, the spots with various shades of red were regularly distributed on the microarray (Supplementary Fig. 2). The visualization of the results was achieved by summarizing the gray-scale value of digital images of the stained hydrogel spots (details were presented in "Methods"). We highlight the relatively high value in the three-dimensional histogram with the color red while blue and gray were used to exhibit middle and low values, respectively. As shown in Fig. 6a, two trends were observed following immersion of the hydrogel coating microarrays with Congo red solution. Generally, the drug-loading capacity of hydrogel coating correlates positively with the ratio of SBMA in monomers. Substituting HEMA with SBMA in monomers renders the more red columns in the group of hydrogel microarrays with the crosslinker PEGDMA

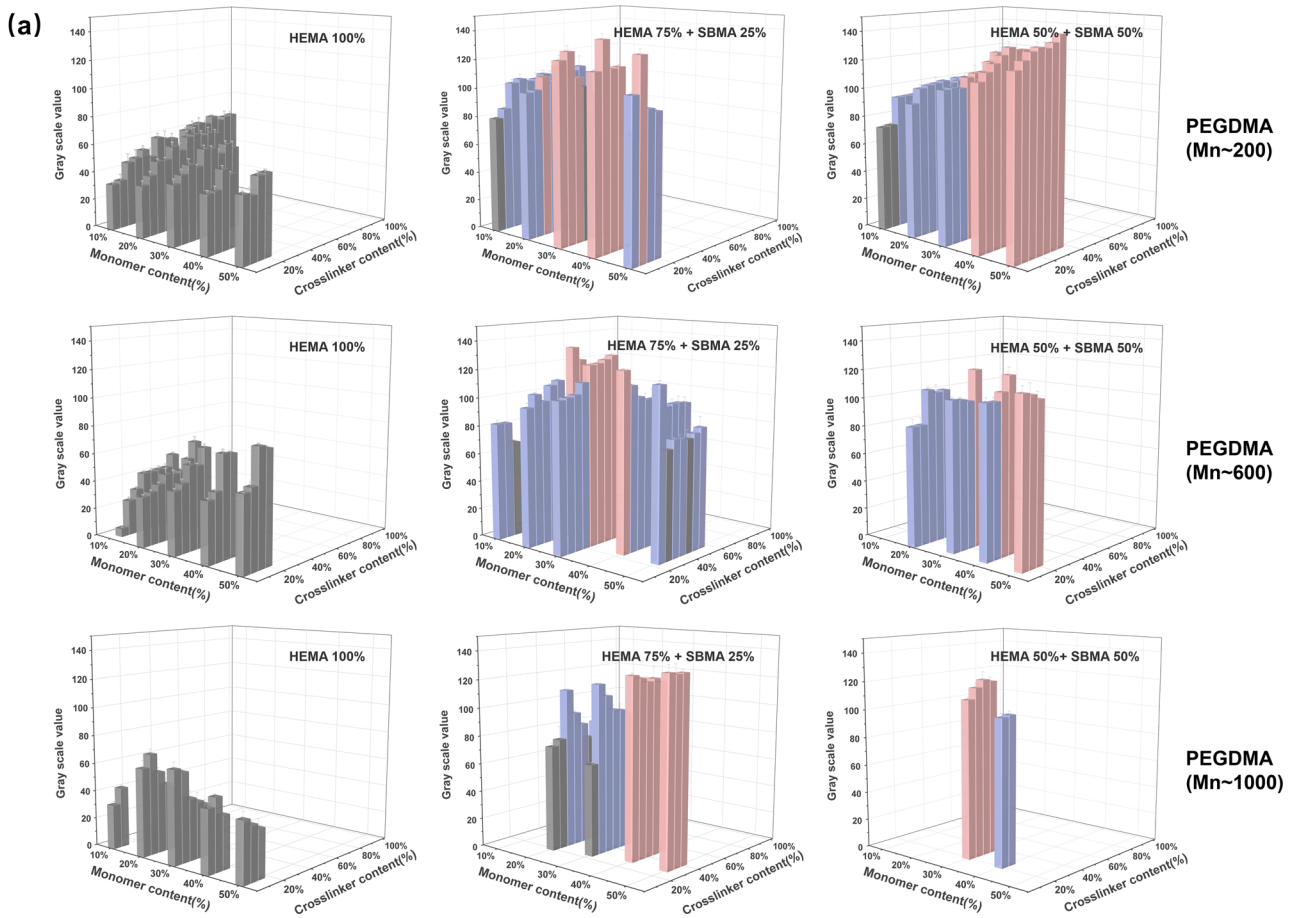

Fig. 6 The drug-loading capacity test results of the hydrogel microarrays via a high-throughput manner. a Quantification of the color depth of each hydrogel coating spot after immersion in Congo red solution for 24 h. The red columns represent the spots with the gray-scale value more than 110; the blue columns represent the spots with the gray-scale value ranging from 80 to 110; the gray columns represent the spots with the gray-scale value less than 80. The gray-scale value correlates positively with the color depth of hydrogel spots. **b** Final selection of hydrogel coating spots with optimized stability and drug-loading capacity.

(Mn ~200). In addition, another clear trend was observed within the group with the same monomer composition. Taking (HEMA: SBMA = 75%: 25%; 20% monomer; crosslinker Mn ~600)-hydrogel microarray as an example, the drug-loading capacity of hydrogel spots first increased and then decreased as the content of crosslinker increased. This trend is attributed to that higher crosslinker content rendered the hydrogel spot less swellable, and therefore worse drug-loading capacity than a spot with a lower crosslinker content. But excessively low crosslinker content led to the inadequate mechanical stability of the hydrogel network, which lowered the swellability of the hydrogel spots. Therefore, the high SBMA ratio and low crosslinker content were exhibited to contribute to good drug-loading capacity, which was consistent with the results obtained from bulk hydrogels in previous works[43,44]. Typically, the high SBMA ratio in monomers may contribute to good antifouling ability of hydrogel coatings. SBMA segments could accommodate more water molecules around polymer chains via hydrogen bonding and ionic solvation[45]. Inadequate elastic properties of the hydrogel network owing to excessively low crosslinker would lead to poor antifouling ability[46]. Moreover, the screening results of the drug-loading capacity also helped to identify the antifouling ability of the coatings. The antimicrobial/antifouling drugs loaded in hydrogel coatings would contribute to their antifouling ability. Finally, the high-throughput

combinatorial synthesis and characterization strategy rapidly screened 10 out of 1575 hydrogel coating formulations in the given conditions (Fig. 6b).

DISCUSSION

In summary, an efficient method that combines highly miniaturized hydrogel synthesis and characterization was employed to design antifouling coatings with optimized stability and drug-loading capacity. Benefiting from the picoliter droplet microarrays printed by non-contact liquid-dispensing technology, the hydrogel coatings with 1575 different compositions were rapidly produced, which only required 0.6 mL reactant in total and 150 min. A continuous gradient of both SBMA and HEMA ratio in monomers, crosslinker content with respect to monomers, the molecular weight of crosslinker as well as monomer contents were produced by overprinting different volumes of these compounds along the abscissa and ordinate axis of the microarray. The hydrogel coating microarrays were used for subsequent high-throughput biological screening.

During the production of hydrogel coating microarrays, a vortex was generated during the print of each droplet to ensure the adequate mixing of the components, which was confirmed by Raman spectroscopy and fluorescence measurement. The mechanical stability of each spot in microarrays was assessed by immersion swelling as well as flow and tape-peeling tests. The results demonstrated correlations between the synthesis parameters and the stability of hydrogel coatings. The hydrogel coating microarrays were stained with Congo red to quantitatively assess the drug-loading capacity, which increased with a high SBMA ratio and low crosslinker content. Finally, 10 out of 1575 SBMA/HEMA hydrogel coatings stood out via the high-throughput screening strategy proposed in this study. Our approach enables the rapid identification of optimal synthesis parameters from an immense combinatorial space, thereby facilitating the fine design of biomaterial surfaces.

METHODS

Material

316 L stainless substrates with a size of $80 \times 60 \times 1$ mm were abraded continuously by 400, 800, and 1200 grit abrasive papers. The well-abraded samples were cleaned in ethanol under ultrasonication and subsequently dried by argon before use. 2-Hydroxyethyl methacrylate (HEMA) and sulfobetaine methacrylate (SBMA) were purchased from Sigma-Aldrich. Poly (ethylene glycol) dimethacrylate (PEGDMA) (Mn ~200, 600, and 1000), 2-hydroxy-4′-(2-hydroxyethoxy)-2-methylpropiophenone, fluorescein, rhodamine B and Congo red were purchased from Aladdin Industrial Corporation. All reagents were used as received without further purification.

Synthesis of hydrogel microarrays

An automated non-contact droplet microarray printer (Nano-PlotterTM NP2.1, Germany) was used to achieve the software-controlled droplet dispensing. The viscosity of aqueous monomer stock solutions was adjusted via a heating system to reproducibly print droplets on various substrates. We set the volume of a single drop burst to 400 pL and adjusted the number of drops of each component in the software as required before the printing process. The dosage of the solutions was optimized and verified before and after the dispensing process, ensuring precise picoliter-level printing. The ambient humidity was maintained at 70% in the printing procedures.

In a typical solution printing procedure: (i) printing of 50 nL SBMA (1 g mL^{-1} in PBS) on the substrate (30 °C); (ii) overprinting 50 nL with HEMA (1 g mL^{-1} in PBS, 35 °C); overprinting with crosslinker PEGDMA (Mn ~600) with the volume ascending from 0 to 100 nL per spot (step size 5%, 75 °C); iii) overprinting with photoinitiator (2 wt.% in PBS) with a constant volume of 200 nL (25 °C). After these three printing steps, the well-printed droplet microarray on the substrate was irradiated (3 min, 60 mW cm^{-2}) for polymerization to produce the hydrogel microarray. The substrate was surrounded by non-woven fabric soaked with PBS to reduce the evaporation of the solution.

Raman spectroscopy tests

Raman spectroscopy was used to confirm the adequate mixing of two monomers in the droplet generated by an automated non-contact printer (WITec alpha300R, Germany). The hydrogel spot was prepared using 50 nL SBMA, 50 nL HEMA, 30 nL PEGDMA, and 200 nL photoinitiator. We used both regular mode and mapping mode to test the hydrogel spot. The excitation laser in this test was set to 532 nm and the wave number ranged from 50 to 4000 cm^{-1}. The mapping was obtained over a 12×12 matrix per hydrogel spot over 90 min. Each spectrum was integrated based on 3 replicates.

Fluorescence tests

The adequate mixing of the two monomers in the droplet was further evaluated by fluorescence microscopy (3DHISTECH, Hungary). Before the printing procedure, we introduced fluorescein and rhodamine B in SBMA and HEMA solutions, respectively. Then, the hydrogel spot was prepared in the same way described in Section “Raman spectroscopy tests”. Fluorescein and rhodamine B were used as dyes to generate green and red fluorescence, respectively. The homogeneity of the monomers in the hydrogel spot was assessed qualitatively by green and red fluorescence, respectively.

Stability tests

The stability of the as-prepared hydrogel spots was sequentially evaluated by immersion swelling, flow and tape-peeling tests. In the immersion swelling test, the hydrogel microarray was placed in a closed petri-dish containing 20 mL PBS and allowed to stand for 72 h. After the immersion, the sample was washed with ethanol for three times to remove the floating hydrogel spots and subsequently dried by argon before characterization. In the flow test, the hydrogel microarray was placed in a closed glass container with a flow rate adjusted to 500 mL min^{-1} using a peristaltic pump (FlexiPump, France) in order to simulate the blood flow rate in an artery[47]. After 72 h of flow tests, the sample was washed and dried in the same fashion as the immersion test. The stability of the as-prepared hydrogel spots was also investigated by the tape-peeling test. In brief, the tapes (3 M, CT-18, 600#) were pressed against the surface of the hydrogel microarray with a force of 50 N and subsequently torn off at an angle of 45°. This procedure was repeated for 10 cycles for each microarray. The morphology of the hydrogel spots after these damage tests was characterized via an optical microscope (Zeiss Axiocam, Germany).

Drug-loading capacity

In order to assess the drug-loading capacity of hydrogel spots, we immersed the hydrogel microarrays in the Congo red solution for 24 h. Subsequently, the samples were taken out and washed with ethanol to remove all dyes attached to the substrate. The hydrogel microarrays were dried with argon before characterization and the digital images of the stained hydrogel microarrays were taken afterward. ImageJ software was used to quantitatively assess the drug-loading capacity of each hydrogel spot, the key steps of which were as follows: (i) converting the original RGB images of microarrays to 8-bit format in order to obtain the gray-scale

images (gray-scale images give values to images according to their color depth; the maximum value is 255, which represents pure white; the minimum one is 0, which represents pure black; and the value between 0–255 represents gray); (ii) inverting the black and white of the images; (iii) calibrating the optical density value; (iv) delineating the target scope, and obtaining the mean gray-scale value.

DATA AVAILABILITY

The raw data are available from the corresponding authors upon reasonable request.

Received: 27 February 2023; Accepted: 3 May 2023;
Published online: 26 June 2023

REFERENCES

1. Pozo, J. L. D. Biofilm-related disease. *Expert Rev. Anti-Infect. Ther.* **16**, 51–65 (2018).
2. Bjarnsholt, T. et al. The in vivo biofilm. *Trends Microbiol.* **21**, 466–474 (2013).
3. Anderson, J. M. Future challenges in the in vitro and in vivo evaluation of biomaterial biocompatibility. *Regen. Biomater.* **3**, 73–77 (2016).
4. Darouiche, R. O. Treatment of infections associated with surgical implants. *N. Engl. J. Med.* **350**, 1422–1429 (2004).
5. Lemiech-Mirowska, E., Kiersnowska, Z. M., Michalkiewicz, M., Depta, A. & Marczak, M. Nosocomial infections as one of the most important problems of healthcare system. *Ann. Agric. Environ. Med.* **28**, 361–366 (2021).
6. Seliktar, D. Designing cell-compatible hydrogels for biomedical applications. *Science* **336**, 1124–1128 (2012).
7. Fu, M. J. et al. Recent advances in hydrogel-based anti-infective coatings. *J. Mater. Sci. Technol.* **85**, 169–183 (2021).
8. Lin, C.-C. & Anseth, K. S. PEG hydrogels for the controlled release of biomolecules in regenerative medicine. *Pharm. Res.* **26**, 631–643 (2009).
9. Zare, M. et al. pHEMA: An overview for biomedical applications. *Int. J. Mol. Sci.* **22**, 6376 (2021).
10. Li, Q. S. et al. Zwitterionic biomaterials. *Chem. Rev.* **122**, 17073–17154 (2022).
11. Jiang, S. Y. & Cao, Z. Q. Ultralow-fouling, functionalizable, and hydrolyzable zwitterionic materials and their derivatives for biological applications. *Adv. Mater.* **22**, 920–932 (2010).
12. He, M. R. et al. Zwitterionic materials for antifouling membrane surface construction. *Acta Biomater.* **40**, 142–152 (2016).
13. Kondo, T. et al. Structure of water at zwitterionic copolymer film–liquid water interfaces as examined by the sum frequency generation method. *Colloids Surf. B* **113**, 361–367 (2014).
14. Chang, Y. et al. Tunable bioadhesive copolymer hydrogels of thermoresponsive poly(N-isopropyl acrylamide) containing zwitterionic polysulfobetaine. *Biomacromolecules* **11**, 1101–1110 (2010).
15. Gong, Y. K., Liu, L. P. & Messersmith, P. B. Doubly biomimetic catecholic phosphorylcholine copolymer: a platform strategy for fabricating antifouling surfaces. *Macromol. Biosci.* **12**, 979–985 (2012).
16. Huang, T. et al. Zwitterionic copolymers bearing phosphonate or phosphonic motifs as novel metal-anchorable anti-fouling coatings. *J. Mat. Chem. B* **5**, 5380–5389 (2017).
17. Kim, S. H., Kim, S.-H., Nair, S. & Moore, E. Reactive electrospinning of crosslinked poly(2-hydroxyethyl methacrylate) nanofibers and elastic properties of individual hydrogel nanofibers in aqueous solutions. *Macromolecules* **38**, 3719–3723 (2005).
18. Moghadam, M. N. & Pioletti, D. P. Improving hydrogels' toughness by increasing the dissipative properties of their network. *J. Mech. Behav. Biomed. Mater.* **41**, 161–167 (2015).
19. Kim, S., English, A. E. & Kihm, K. D. Surface elasticity and charge concentration-dependent endothelial cell attachment to copolymer polyelectrolyte hydrogel. *Acta Biomater.* **5**, 144–151 (2009).
20. Dulong, V. et al. Hyaluronan-based hydrogels particles prepared by crosslinking with trisodium trimetaphosphate. *Carbohydr. Polym.* **57**, 1–6 (2004).
21. Yang, J. et al. Mechanically durable antibacterial nanocoatings based on zwitterionic copolymers containing dopamine segments. *J. Mater. Sci. Technol.* **89**, 233–241 (2021).
22. Griner, L. A. M., Guha, R., Shinn, P. & Thomas, C. J. High-throughput combinatorial screening identifies drugs that cooperate with ibrutinib to kill activated B-cell–like diffuse large B-cell lymphoma cells. *Proc. Natl Acad. Sci. USA* **111**, 2349–2354 (2014).
23. Wang, C. et al. A facile method for high-throughput screening of drug-eluting coatings in droplet microarrays based on ultrasonic spray deposition. *Biomater. Sci.* **9**, 6787–6794 (2021).
24. Lei, W. et al. Droplet-microarray: miniaturized platform for high-throughput screening of antimicrobial compounds. *Adv. Biosyst.* **4**, e2000073 (2020).
25. Fang, Z. et al. High-throughput screening and rational design of biofunctionalized surfaces with optimized biocompatibility and antimicrobial activity. *Nat. Commun.* **12**, 3757 (2021).
26. Wu, J. et al. Importance of zwitterionic incorporation into polymethacrylate-based hydrogels for simultaneously improving optical transparency, oxygen permeability, and antifouling properties. *J. Mater. Chem. B* **5**, 4595–4606 (2017).
27. Yang, B. & Yuan, W. Highly stretchable, adhesive, and mechanical zwitterionic nanocomposite hydrogel biomimetic skin. *ACS Appl. Mater. Interfaces* **11**, 40620–40628 (2019).
28. Wang, S. et al. Mussel-inspired adhesive zwitterionic composite hydrogel with antioxidant and antibacterial properties for wound healing. *Colloids Surf. B* **220**, 112914 (2022).
29. Yao, M. et al. Microgel reinforced zwitterionic hydrogel coating for blood-contacting biomedical devices. *Nat. Commun.* **13**, 5339 (2022).
30. Shen, J., Du, M., Wu, Z., Song, Y. & Zheng, Q. Strategy to construct polyzwitterionic hydrogel coating with antifouling, drag-reducing and weak swelling performance. *RSC Adv.* **9**, 2081–2091 (2019).
31. Zhang, H. et al. Tough physical double-network hydrogels based on amphiphilic triblock copolymers. *Adv. Mater.* **28**, 4884–4890 (2016).
32. Wang, M. et al. Rapid self-recoverable hydrogels with high toughness and excellent conductivity. *ACS Appl. Mater. Interfaces* **10**, 26610–26617 (2018).
33. Jiang, Z. et al. Robust hydrogel adhesive with dual hydrogen bond networks. *Molecules* **26**, 2688 (2021).
34. Chou, F. et al. Ultra-low fouling and high antibody loading zwitterionic hydrogel coatings for sensing and detection in complex media. *Acta Biomater.* **40**, 31–37 (2016).
35. Tran, V. T., Mredha, M. T. I. & Jeon, I. High-water-content hydrogels exhibiting superior stiffness, strength, and toughness. *Extrem. Mech. Lett.* **37**, 100691 (2020).
36. Dong, L. et al. Hydrogel antifouling coating with highly adhesive ability via lipophilic monomer. *Macromol. Mater. Eng.* **307**, 2100812 (2022).
37. Iwasaki, K. et al. Bioengineered three-layered robust and elastic artery using hemodynamically-equivalent pulsatile bioreactor. *Circulation* **118**, S52–S57 (2008).
38. Zhang, F. et al. Superhydrophobic carbon nanotubes/epoxy nanocomposite coating by facile one-step spraying. *Surf. Coat. Tech.* **341**, 15–23 (2018).
39. Osaheni, A. O., Finkelstein, E. B., Mather, P. T. & Blum, M. M. Synthesis and characterization of a zwitterionic hydrogel blend with low coefficient of friction. *Acta Biomater.* **46**, 245–255 (2016).
40. Wei, Q., Cai, M., Zhou, F. & Liu, W. Dramatically tuning friction using responsive polyelectrolyte brushes. *Macromolecules* **46**, 9368–9379 (2013).
41. Adibnia, V., Olszewski, M., Crescenzo, G. D., Matyjaszewski, K. & Banquy, X. Superlubricity of zwitterionic bottlebrush polymers in the presence of multivalent ions. *J. Am. Chem. Soc.* **142**, 14843–14847 (2020).
42. Tronci, V. G., Ajiro, H., Russell, S. J., Wood, D. J. & Akashi, M. Tunable drug-loading capability of chitosan hydrogels with varied network architectures. *Acta Biomater.* **10**, 821–830 (2014).
43. Rosenfeld, A., Oelschlaeger, C., Thelen, R., Heissler, S. & Levkin, P. A. Miniaturized high-throughput synthesis and screening of responsive hydrogels using nanoliter compartments. *Mater. Today Bio.* **6**, 100053 (2020).
44. Jung, S., Park, S., Choi, D. & Hong, J. Efficient drug delivery carrier surface without unwanted adsorption using sulfobetaine zwitterion. *Adv. Mater. Interfaces* **7**, 2001433 (2020).
45. He, H. et al. Importance of zwitterionic incorporation into polymethacrylate-based hydrogels for simultaneously improving optical transparency, oxygen permeability, and antifouling properties. *J. Mater. Chem. B* **5**, 4595–4606 (2017).
46. Wu, J. et al. Zwitterionic poly(sulfobetaine methacrylate) hydrogels with optimal mechanical properties for improving wound healing in vivo. *J. Mater. Chem. B* **7**, 1697–1707 (2019).
47. Obiweluozor, F. O. et al. Thromboresistant semi-IPN hydrogel coating: Towards improvement of the hemocompatibility/biocompatibility of metallic stentimplants. *Mat. Sci. Eng. C.* **99**, 1274–1288 (2019).

ACKNOWLEDGEMENTS

The work was financially supported by the National Key Research and Development Program of China (2022YFB3808803).

AUTHOR CONTRIBUTIONS

D.Z. and J.Y. conceived the study. J.Y., Y.R., and L.H. drafted the manuscript and conducted the experiments under the supervision of D.Z. All authors evaluated and analyzed the results. D.Z., L.M., and X.H. reviewed and edited the paper.

COMPETING INTERESTS

The authors declare no competing interests.

ADDITIONAL INFORMATION

Supplementary information The online version contains supplementary material available at https://doi.org/10.1038/s41529-023-00362-5.

Correspondence and requests for materials should be addressed to Dawei Zhang.

Reprints and permission information is available at http://www.nature.com/reprints

Publisher's note Springer Nature remains neutral with regard to jurisdictional claims in published maps and institutional affiliations.